# Optimization of Multiparametric Flow Cytometry Assays: A Comprehensive Assessment of Immunophenotypic Characteristics of Monocytic and Blastic Plasmacytoid Dendritic Cell Neoplasms

Jung Heard

A thesis

submitted in partial fulfillment of the

requirements for the degree of

Master of Science

University of Washington

2024

Committee:

Sindhu Cherian

Jonathan Fromm

David Wu

Program Authorized to Offer Degree:

Laboratory Medicine

University of Washington

## Abstract

Optimization of Multiparametric Flow Cytometry Assays:

A Comprehensive Assessment of Immunophenotypic Characteristics

of Monocytic and Blastic Plasmacytoid Dendritic Cell Neoplasms

Jung Heard

Chair of the Supervisory Committee:

Sindhu Cherian

Department of Laboratory Medicine and Pathology

This study aimed to design and optimize multiparametric flow cytometry (MFC) assays for in-depth characterization of monocytic cells and plasmacytoid dendritic cells (pDCs) in the context of hematological neoplasms, such as monocytic leukemia and blastic plasmacytoid dendritic cell neoplasm (BPDCN). Building on previous research, we integrated novel markers, including LILRB1, LILRB4, and CD300e for the monocytic assay panel and CD303 and CD304 for the pDC assay panel, to provide a comprehensive characterization of antigenic expression associated with maturation and differentiation of these populations. We established unique expression patterns of novel markers and highlighted distinctive immunophenotypic features of monocytic cells and pDCs in their normal and neoplastic state, demonstrating robust performance and reliability of the optimized assays.

## Table of Contents

## 1. Introduction:

Multiparametric flow cytometry (MFC) has long served as one of the essential tools in the diagnosis of hematological neoplasms.[1] The efficacy of MFC is largely attributed to its ability to provide relatively rapid results, as well as its wide selection of monoclonal antibodies.[1–3] Prompt turnaround time in obtaining test results is critical as timely initiation of treatment can significantly influence patient outcomes. Additionally, MFC offers unique capabilities for comprehensive immunophenotypic profiling at a single-cell level, which enable accurate classification of leukemic cells, leading to precise diagnosis and stratification of prognosis.

Nevertheless, the flow cytometric evaluation of monocytic neoplasms and blastic plasmacytoid dendritic cell neoplasm (BPDCN) remain diagnostic challenges due to the lack of sensitive and specific markers for monocytic and plasmacytoid dendritic cells (pDCs).[4–7] Furthermore, the absence of definitive genetic markers for the diagnosis of monocytic neoplasms and BPDCN emphasizes the importance of immunophenotyping by MFC in these entities.[8] Consequently, the primary objective of this study is to optimize MFC assays for a comprehensive immunophenotypic characterization for monocytes and pDCs, thereby enhancing diagnostic precision. In the following sections, the complexities and challenges of current flow cytometric assessment of monocytic neoplasms and BPDCN will be discussed with emphasis on potential benefits of incorporating novel markers in mitigating diagnostic challenges.

### 1.1 Monocytic Neoplasm

Monocytic neoplasm can manifest as acute or chronic phase. In the absence of defining genetic or clinical data, current World Health Organization (WHO) and International Consensus

Classification (ICC) guidelines classify acute myeloid leukemia with monocytic differentiation (M-AML) into two subcategories, acute myelomonocytic leukemia and acute monocytic leukemia, which are primarily differentiated based on the proportion of monocytes and their precursors.[8,9] Additionally, chronic myelomonocytic leukemia (CMML) represents the most common entity within the myelodysplastic syndrome/myeloproliferative neoplasm (MDS/MPN) category characterized by persistent monocytosis in peripheral blood (PB) with various somatic mutations.[10] Clinical features frequently associated with monocytic neoplasms include cutaneous and gingival infiltrations, bleeding disorders, extramedullary masses, and central nervous system (CNS) involvement, which require different clinical interventions than other myelogenous leukemia subtypes, highlighting the importance of accurate diagnosis.[4,6]

Currently, several myelomonocytic markers are utilized for evaluating monocytic cells at the University of Washington hematopathology laboratory (UWHL, Seattle, USA), including CD13, CD14, CD15, CD16, CD33, and CD64, each carrying their own diagnostic strengths and limitations. Nevertheless, it is often challenging to accurately delineate immature monocytes among the heterogeneous mixture of hematopoietic cells due to the absence of lineage defining markers for immature monocytic markers and the overlapping immunophenotypic characteristics with granulocytic cells. CD14, for instance, is a relatively specific marker for mature monocytes expressed at a high intensity; however, its utility as a sensitive monocytic marker is compromised by its dim to absent expression on immature monocytes.[11] Chen at al., previously reported that high levels of CD14 on maturing granulocytic cells are frequently observed in patients with myeloid neoplasms with monosomy 7 and post-granulocyte colony stimulating factor (G-CSF) treatment.[12] Consequently, a combination of antigens, such as CD33 and CD64, are used to

enhance sensitivity; nonetheless, their specificity remains limited due to varying intensities expressed on maturing granulocytic cells.[11,12] Such immunophenotypic complexities and limitations of current flow cytometric methods underscore the imperative need for an optimized MFC assay for precise classification and diagnosis of hematologic neoplasms.

Recent studies highlight three novel monocytic markers, LILRB1, LILRB4, and CD300e, which have demonstrated potential for providing detailed immunophenotypic characteristics and complete maturation patterns of monocytic cells.[4,11,13,14] Churchill et al. and Dobrowlska et al. described the potential diagnostic usefulness of two novel markers, LILRB1 and LILRB4 (leukocyte immunoglobulin-like receptor B 1 and 4), also known as ILT2 and ILT3 (immunoglobulin-like transcripts 2 and 3), respectively.[11,13] Co-expression of LILRB1 and LILRB4 at all stages of monocytic maturation suggests their potential as useful diagnostic markers as these markers are expressed in immature monocytic cells prior to the acquisition of CD14 expression. The studies further highlight the diagnostic implication of LILRB1 and LILRB4 as highly specific monocytic lineage defining markers for distinguishing M-AML from other AML subtypes as these two markers are consistently expressed on monocytic cells at all stages of maturation even in the neoplastic conditions. Such a finding is particularly relevant as these markers are essentially absent in myeloblasts and myeloid populations under both normal and neoplastic conditions. For instance, the microgranular variant of acute promyelocytic leukemia (APL) warrants careful flow cytometric assessment due to the atypical immunophenotypic and morphologic presentations.[15] The investigations elucidated that LILRB1 and LILRB4 significantly improved diagnostic confidence in differentiating microgranular variant APL from the background immature monocytic population.[13] CD300e (immune receptor expressed by myeloid cells-2 or

IREM-2) has also shown clinical utility as a monocytic marker.[4,14] According to the studies, CD300e expression peaks in late-stage monocytic maturation and demonstrates its specificity in classifying monocytic subsets. In this context, we designed an 11-color MFC monocytic assay and examined how the integration of LILRB1, LILRB4, and CD300e with other useful myelomonocytic markers may contribute to the diagnostic value of the assay.

**1.2 Blastic plasmacytoid dendritic cell neoplasm (BPDCN)**

Similar to the challenges encountered in diagnosing monocytic neoplasms, BPDCN also presents its own unique set of obstacles. BPDCN is a rare and aggressive hematopoietic neoplasm originating from pDC precursors.[7] Historically, BPDCN has been known by various titles due to the nature of ambiguous morphologic and immunophenotypic features. However, in line with medical advancements, the 2016 revision of the WHO classification clearly categorized BPDCN as an independent entity, distinguishing it from AML subtype.[16] Additionally, the 2022 WHO and ICC updates further emphasized this distinction of BPDCN, highlighting the significance of immunophenotypic diagnostic criteria.[8,9] BPDCN typically manifests with multi-site involvement, most commonly affecting the skin, bone marrow (BM), PB, and lymph nodes.[17] Diagnosis is generally made based on the combination of clinical presentation, morphologic features, and immunophenotypic characteristics.

By flow cytometry, normal pDCs are typically found in the CD45 versus side scatter (SSC) defined blast gate and identified by positive expression of CD4, CD38, bright CD123, and HLA-DR with the absence of other myelomonocytic or lymphoid lineage-specific markers.[18] The expression of

CD56 is often used to distinguish neoplastic pDCs coupled with decreased CD38, decreased CD123 and bright HLA-DR, though CD56 can also be found in a small subset of reactive pDCs. Although the current WHO guidelines provide comprehensive immunophenotypic diagnostic criteria, the classification of BPDCN can be challenging due to the variability in marker expression in neoplastic pDCs, as well as the presence of CD56+ reactive pDCs often observed in post-therapy samples. Additionally, the emergence of immunotherapies targeting CD123 for BPDCN underscores the need for additional pDC-specific markers, necessitating the development of an optimized MFC assay.

A recent study by Wang et al. demonstrated that using a combination of 10 markers, CD2, CD4, CD7, CD38, CD45, CD56, CD64, CD123, CD303, and HLA-DR, effectively distinguished between CD56+ neoplastic pDCs and background normal and CD56+ reactive pDCs.[19] The findings suggest that immunophenotypic features of CD56+ reactive pDCs were distinctive from normal and neoplastic counterparts, consistently expressing positive CD2, negative CD7, and uniformly bright CD38. In contrast, CD56+ BPDCN cells frequently express negative CD2 (81%), positive CD7 (64%) with decreased CD38 expression. As for new pDC-specific marker consideration, several studies highlighted CD303 and CD304 (blood dendritic cell antigens BDCA-2 and BDCA-4, respectively) for improved diagnostic confidence and enhanced therapeutic approaches. [7,8,17,19,20] These markers have been confirmed to be specific towards pDCs, thus providing potential implications for the development of an optimized MFC assay.

In light of current diagnostic challenges for monocytic neoplasms and BPDCN by MFC, our study aims to design and validate a set of MFC assays with incorporation of novel markers, LILRB1,

LILRB4, and CD300e for the monocytic assay and CD303 and CD304 for the pDC assay. We hypothesize that the optimized monocytic and pDC assays can provide substantial improvement in diagnostic precision and accuracy.

## 2. Materials and Methods

### 2.1 Case identification and sample selection

The monocytic and pDC assay optimization studies were conducted at the University of Washington Hematopathology Laboratory (UWHL, Seattle, WA) between 7/20/2022 and 8/12/2023. All samples utilized in this assay optimization study constituted left over material and were selected after clinical diagnostic workup was finalized. All samples were deidentified prior to the study. Validation samples selected for this study were based on the presence of monocytic or dendritic cell populations identified during the course of routine clinical laboratory work. Of note, sample type, collection date, collection tube type, diagnosis, disease stage, and final flow cytometry reports were collected to facilitate a clear and comprehensive evaluation for this study. The sample types included BM, PB, and cerebrospinal fluid (CSF, monocytic assay only). Additionally, this study was granted exemption by the University of Washington's Institutional Review Board (UW IRB, Seattle, WA) due to the utilization of de-identified samples, ensuring compliance with all relevant ethical considerations. The process and its approval are documented and recorded during the IRB consultation.

#### Monocytic assay sample selection

A total of 50 samples were selected based on three main sample selection criteria, which include normal control (n=11, BM=9, PB=2), reactive monocytosis (n=10, BM=7, PB=3), and leukemia

cases (n=26 BM=12, PB=14). Normal control samples were those without detectable diseases by MFC, morphology, and other detection methods. Reactive monocytosis cases were identified by a significant increase in monocytic population (>10% of total WBCs) without other abnormal findings. Abnormal leukemia samples were identified from five different leukemia subtypes for differential studies: AML (n=8), M-AML (n=10), APL (n=3), CMML (n=4), and BPDCN (n=1). Additionally, CSF (n=3) samples are included for monocytic assay evaluation **(Table 1)**.

**Table 1**: Monocytic Assay Validation Sample Selection Criteria and Total Sample Count

| **Diagnosis** | **No. of Cases (BM/PB)** |
|---|---|
| Normal control cases | 11 (9/2) |
| Reactive monocytosis (>10% monocytes/ WBCs) | 10 (7/3) |
| Acute myeloid leukemia (AML) | 8 (4/4) |
| AML with monocytic differentiation (M-AML) | 10 (5/5) |
| Acute promyelocytic leukemia (APL) | 3 (0/3) |
| Chronic myelomonocytic leukemia (CMML) | 4 (3/1) |
| Blastic plasmacytoid dendritic cell neoplasm (BPDCN) | 1 (1/0) |
| Cerebrospinal fluid (CSF) | 3 |
| **Total cases used for validation** | **50** |

**pDC assay sample selection**

A total of 27 BM an PB samples were obtained for this study. The normal control samples (n=17, BM=15, PB=2) include post-diagnostic samples without detectable hematological abnormalities. Out of these 17 normal control cases, we identified 5 cases that containing subset of CD56+ reactive pDCs for the pDC assay validation study. Of note, those cases containing CD56+ reactive pDCs with less than 50 events were considered not present and excluded from further assessment during the data analysis to ensure the accuracy and reliability of the data. BPDCN (n=10, BM=8,

PB=2; 2 samples from same patient on same day BM/PB collection, post-therapy) samples were obtained from those newly diagnosed or relapsed cases **(Table 2)**.

**Table 2:** pDC Assay Validation Sample Selection Criteria and Total Sample Count.

| **Diagnosis** | **No. of Cases (BM/PB)** |
|---|---|
| Normal (5 cases include CD56+ reactive pDCs) | 17 (15/2) |
| Blastic Plasmacytoid dendritic cell neoplasm (BPDCN) | 10 (8/2) |
| **Total cases used for validation** | **27** |

### 2.2 Monoclonal antibody selection

Monoclonal antibodies for each assay panel were selected based on the foundational elements essential to robust MFC assay development. A thoughtfully designed and optimized MFC assay should offer clear classification of blasts or blast equivalents, provide in-depth immunophenotypic profiling and maturation stages, and distinguish aberrant phenotypic expression unique to the target cell population. In this regard, we concentrated on three specific criteria for antibody selection: 1) backbone markers, 2) lineage-specific markers, and 3) frequently expressed aberrant markers. Consequently, the monocytic and the pDC assays share four backbone markers with current routine myeloid assays used at the UWHL, which include CD34, CD38, CD45, and HLA-DR to facilitate precise identification of blast and blast equivalents across the assays.

#### Monocytic assay monoclonal antibody selection

11-color monocytic assay is comprised of four backbone markers, CD34, CD38, CD45, and HLA-DR, four monocyte-associated markers, CD14, CD16, CD33, and CD64 with the addition of the

three novel monocytic markers of interest, LILRB1, LILRB4 and CD300e. A detailed description of the monoclonal antibody list for monocytic assay is available in **Table 3**.

**Table 3: 11-Color Monocytic Assay Monoclonal Antibody List**

| Antibody | Fluorochrome | Titer(µL) | Clone | Vendor | Catalog No. |
|---|---|---|---|---|---|
| **CD14** | BV786 | 5 | M5E2 | Becton-Dickinson | 563698 |
| **CD16** | BV605 | 5 | 3G8 | Becton-Dickinson | 563172 |
| **CD33** | BV711 | 2 | P67.6 | BioLegend | 366624 |
| **CD34** | APC-R700 | 5 | 8G12 | Becton-Dickinson | 659114 |
| **CD38** | BV510 | 2 | HB-7 | BioLegend | 356612 |
| **CD45** | APC-H7 | 5 | 2D1 | Becton-Dickinson | 641408 |
| **CD64** | FITC | 20 | 22 | Beckman Coulter | IM1604U |
| **CD300e** | APC | 5 | UP-H2 | Becton-Dickinson | 656159 |
| **HLA-DR** | PB | 10 | IMMU-357 | Beckman Coulter | A74781 |
| **LILRB-1** | PE-Cy7 | 5 | HP-F1 | eBioscience | 25-5129-42 |
| **LILRB-4** | PE | 5 | ZM4.1 | eBioscience | 12-5139-42 |

**Abbreviations:** HLA-DR (human leukocyte antigen-DR), LILRB (leukocyte immunoglobulin like receptor B), BV786 (Brilliant™ Violet 786), BV605 (Brilliant™ Violet 605), BV711 (Brilliant™ Violet 711), APC-R700 (allophycocyanin-R700), BV510 (Brilliant™ Violet 510), APC-H7 (allophycocyanin-H7), FITC (fluorescein isothiocyanate), APC (allophycocyanin), PB (Pacific Blue), PE-Cy7 (phycoerythrin cyanine-7), and PE (phycoerythrin).

**pDC assay monoclonal antibody selection**

12-color pDC assay incorporates four backbone markers, CD34, CD38, CD45, and HLA-DR, and five differential markers, CD2, CD4, CD7, CD56, and CD64. Additionally, three pDC-associated markers are included for improved specificity: CD123 and two novel markers, CD303 and CD304. A detailed description of the monoclonal antibodies for pDC assay is available in **Table 4**.

**Table 4: 12-Color pDC Assay Monoclonal Antibody List**

| Antibody | Fluorochrome | Titer(µL) | Clone | Vendor | Catalog No. |
|---|---|---|---|---|---|
| **CD2** | APC | 5 | L303.1 | Becton-Dickinson | 341023 |
| **CD4** | BV605 | 5 | RPA-T4 | Becton-Dickinson | 562658 |
| **CD7** | PE-Cy7 | 5 | M-T701 | Becton-Dickinson | 564019 |
| **CD34** | PE-Cy5.5 | 20 | 8G12 | Becton-Dickinson | 347203 |
| **CD38** | BV510 | 2 | HB-7 | BioLegend | 356612 |
| **CD45** | APC-H7 | 5 | 2D1 | Becton-Dickinson | 641408 |
| **CD56** | BV786 | 5 | NCAM16.2 | Becton-Dickinson | 564058 |
| **CD64** | FITC | 20 | 22 | Beckman Coulter | IM1604U |
| **CD123** | PE | 5 | 7G3 | Becton-Dickinson | 554529 |
| **CD303** | BV711 | 5 | 201A | BioLegend | 354233 |
| **CD304** | APC-R700 | 5 | U21-1283 | Becton-Dickinson | 566038 |
| **HLA-DR** | PB | 10 | IMMU-357 | Becton-Dickinson | A74781 |

**Abbreviations**: pDC (plasmacytoid dendritic cell), HLA-DR (human leukocyte antigen-DR), APC (allophycocyanin), BV605 (Brilliant™ Violet 605), PE-Cy7 (phycoerythrin cyanine-7), PE-Cy5.5 (phycoerythrin cyanine 5.5), BV510 (Brilliant™ Violet 510), APC-H7 (allophycocyanin-H7), BV786 (Brilliant™ Violet 786), FITC (fluorescein isothiocyanate), PE (phycoerythrin), BV711 (Brilliant™ Violet 711), APC-R700 (allophycocyanin-R700), and PB (Pacific Blue). and

### 2.3 Monoclonal antibody staining methods and data acquisition

Cell surface staining procedure was initiated by adding 100 µL of anticoagulated BM or PB sample containing approximately 1 x $10^6$ white blood cells (WBCs), along with fluorescently labeled monoclonal antibodies as specified per each assay following correct titer volume. The sample and antibody mix were immediately vortexed and incubated in the dark for 15 minutes at room temperature to allow optimal antibody binding. Subsequently, 1.5 mL of buffered NH4Cl solution containing 0.25% formaldehyde was added to the test tube, and the sample was incubated in the dark for an additional 15 minutes at room temperature for red blood cell (RBC) lysis and fixation

of the labeled WBCs. Following the incubation, the sample was centrifuged at 530 relative centrifugal force (RCF) for 5 minutes, and a washing step was performed using 3 mL of phosphate-buffered saline (PBS) containing 0.3% bovine serum albumin (BSA) and the sample was then centrifuged for an additional 5 minutes. After the supernatant was removed, the cell pellet was resuspended in 100 µL of PBS-BSA solution. A minimum of 1.5 x $10^5$ and up to 1 x $10^6$ events were acquired using a FACSLyric 12-color flow cytometer (BD Biosciences, San Jose, CA, USA) and the resulting data were analyzed using Woodlist software (created by Dr. Brent Wood, University of Washington, Seattle, WA, USA). It should be noted that the staining procedure was adjusted to accommodate lower cell counts for a small subset of cases with cell counts below the minimum cut-off value.

**2.4 Data analysis**

To ensure optimal data quality, routine visual evaluation strategies used at the UWHL were employed prior to the comprehensive analysis of both monocytic cells and pDCs. As depicted in **Figure 1**, data evaluation process involved an examination of four main plots to 1) ensure stable data acquisition (**A-a**; CD45 vs event number), 2) exclude doublets (**A-b**; forward scatter area versus height, FSC-A vs FSC-H), and 3) exclude non-viable cells and debris (**A-c**; forward scatter versus side scatter, FSC-A vs SSC-H), and 4) define white blood cell populations (CD45 vs. SSC-H). Finally, myelomonocytic, blast, and lymphocytic gates were defined on a CD45 vs. SSC-H plot, setting the stage for the subsequent analysis as depicted in **Figure 1A**.

Additionally, a systematic six-tier qualitative scoring system was employed to assign intensity levels of the measured markers. The intensity levels were designated as bright, moderate, dim, dim

to negative, negative, and heterogeneous. The thresholds for each level were determined based on the distribution of fluorescence intensities observed in control samples. This approach standardized the interpretation of the flow cytometric data, facilitating the comparison of marker expressions across samples. It's crucial to recognize that exact thresholds can differ based on the markers, cell types under analysis, individual sample conditions, and baseline intensity of the negative internal control population. Additionally, median fluorescence intensity (MFI) was measured for quantification analysis.

**Monocytic assay gating strategy**

Monocytic populations were characterized by relatively bright CD45 expression with intermediate SSC properties and further delineated using a combination of myelomonocytic markers: CD14, CD16, CD33, CD64, and HLA-DR **(Figure 1. A and B)**. Our study focused on four primary monocytic subsets: immature, classical, intermediate, and non-classical monocytes. Immature monocytes were defined by bright CD64 and HLA-DR with dim to absent CD14 expression. Mature monocytic cells were initially identified by moderate to bright CD14, bright CD33, and CD64 and further categorized into three subsets based on varying CD14 and CD16 expressions: classical ($CD14^{++}/CD16^{-}$), intermediate ($CD14^{+}/CD16^{+}$), and nonclassical ($CD14^{dim/-}/CD16^{++}$). Following the optimal isolation of the four monocytic subsets, the expression pattern and intensity level of LILRB1, LILRB4 and CD300e was assessed for further characterization. Additionally, immunophenotypic characteristics of novel markers on other hematopoietic cell populations were assessed if further investigation was determined to have potential diagnostic usefulness.

**pDC assay gating strategy**

pDCs are typically identified and isolated within the CD45 versus SSC defined blast gate expressing intermediate to dim CD45 intensities. The gating strategy for pDCs starts by selecting cells that express bright CD123 and lack CD64 expression. Subsequently, pDCs are further refined by gating for those that are positive for HLA-DR. This step effectively segregates pDCs from basophils, which are characterized by their absence of HLA-DR expression **(Figure 1.C)**. Subsequently, comprehensive analysis was conducted based on the findings from previous study using various marker combinations, including CD2, CD4, CD7, CD38, and CD56, to distinguish between normal, CD56+ reactive, and CD56+ neoplastic pDCs.[19] Additionally, each pDC subset was assessed for the expression of two novel pDC markers, CD303 and CD304, to determine immunophenotypic features.

**2.5 Statistical analysis**

Statistical analyses were performed using the R software (version 4.3.1). Given the non-normal distribution of our data and the unequal and small sample sizes of the groups, non-parametric statistical tests were deemed most appropriate, and the Mann-Whitney U test was used to compare differences in the MFI of various markers between the distinct cell subsets. Comparisons were made between immature, classical, intermediate, and non-classical monocytes, as well as between normal, CD56+ reactive, and BPDCN cells for monocytic and pDC assay evaluation, respectively. A *p*-value of less than 0.05 was considered statistically significant.

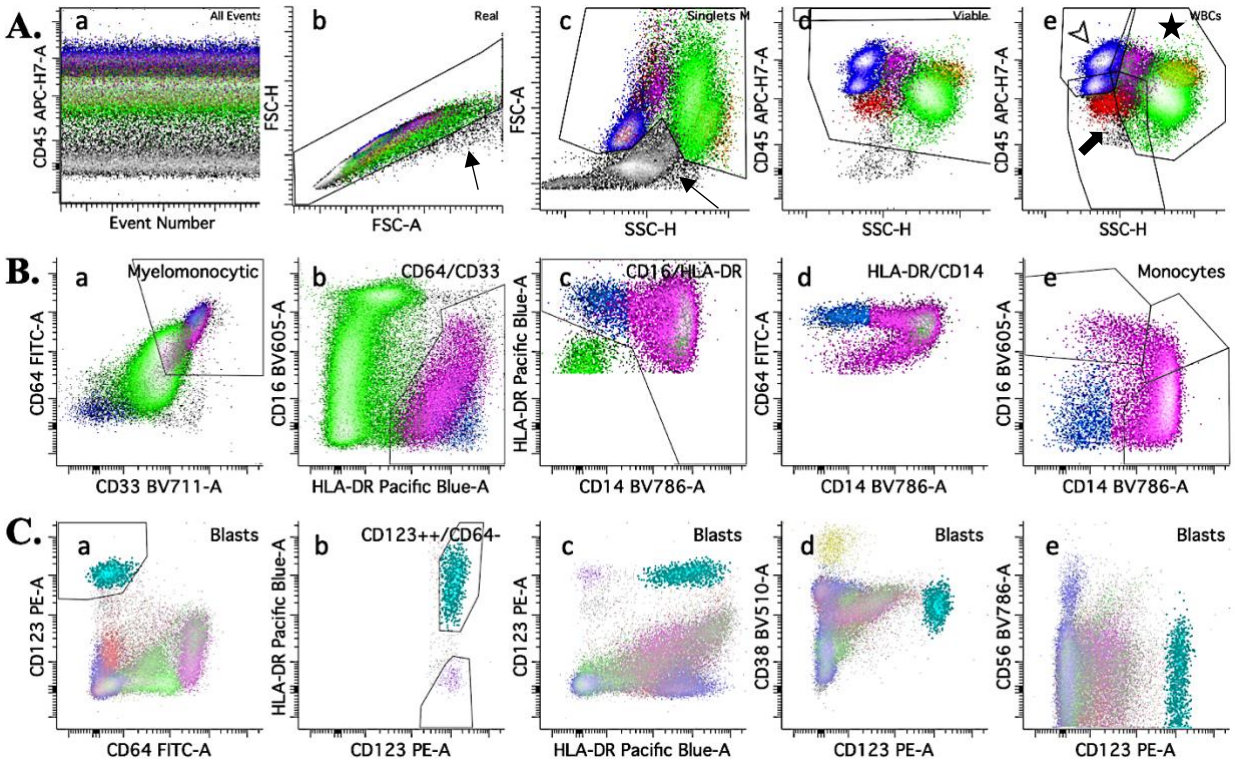


**Figure 1. Systematic approach to data quality evaluation and gating strategies for isolation of monocytic cells and plasmacytoid dendritic cells (pDC) prior to the comprehensive data analysis of new markers.** Above plots showcase the essential steps in MFC data analysis. Application of systematic approaches plays a crucial role in maintaining high quality upstream data, which lays the foundation for precise and accurate downstream interpretations of the cell populations of interest. **Row A: a)** CD45 versus event number plot is used to assess stable data acquisition; **b)** FSC-A vs FSC-H plot is used to exclude doublets (arrow) that may cause erroneous data interpretation; **c)** FSC-A vs. SSC-H plot is utilized for excluding non-viable/dead cells and debris which typically exhibit lower FSC (indicated by an arrow); **d)** CD45 vs. SSC plot is used to define white blood cell populations; **e)** Lymphocytes express brightest CD45 with low SSC (arrowhead), myelomonocytic gate (star) includes both monocytic and granulocytic cells and blast gate (arrow) includes lymphoblasts, myeloblasts, and blast equivalents as well as other WBC populations with low CD45 expression, such as pDCs and basophils. Monocytes (magenta) exhibit

bright CD45 expression and intermediate SSC characteristics, maturing granulocytes (green) show moderate to low CD45 with moderate to high SSC, lymphocytes (blue) are identified by their brightest CD45 and low SSC, and blasts and blast equivalents are characterized by their intermediate to low CD45 with low SSC. **Row B. Initial gating strategy for monocytes:** The process begins with the selection of a monocytic population that is characterized by bright expression of CD33 and CD64 (B-a). This population is then refined by isolating monocytes based on their intermediate to bright expression of HLA-DR, followed by isolation of monocytic cells using HLA-DR versus CD14 plot (B-b, c). Subsequently, a population with dim to absent CD14 expression, indicative of immature monocytes, is isolated for further characterization using novel markers (B-d). The CD16 versus CD14 plot (B-e) delineates further refinement into mature monocytic subsets. **Row C. Initial gating strategy for pDCs**: pDCs (cyan) are first identified by bright CD123 and negative CD64 expression. HLA-DR positivity is then used to refine the pDC population, distinguishing it from HLA-DR negative basophils (purple). Further analysis utilizes a combination of markers CD38 and CD56 to differentiate between normal and CD56+ neoplastic pDC population if present. **Color code:** Row A) dark blue (lymphocytes), magenta (monocytes), green (maturing neutrophils), red (blasts), orange (eosinophils); Row B) blue (immature monocytes), magenta (mature monocytes), green (granulocytes); Row C) cyan (pDCs), purple (basophils), magenta (monocytes), green (granulocytes), red (blasts), yellow (plasma cells), dark blue (lymphocytes).

## 3. Results

### 3.1. Immunophenotypic characteristics of normal, reactive, and leukemic monocytic cells

Our monocytic assay data analysis provided robust maturational profiles and distinct immunophenotypic characteristics in normal cases (n=11, BM=9, PB=2). The line graph below **Figure 2** encapsulates these findings and offers a visual comparison of marker expressions that set the foundation for in-depth discussions in subsequent sections.

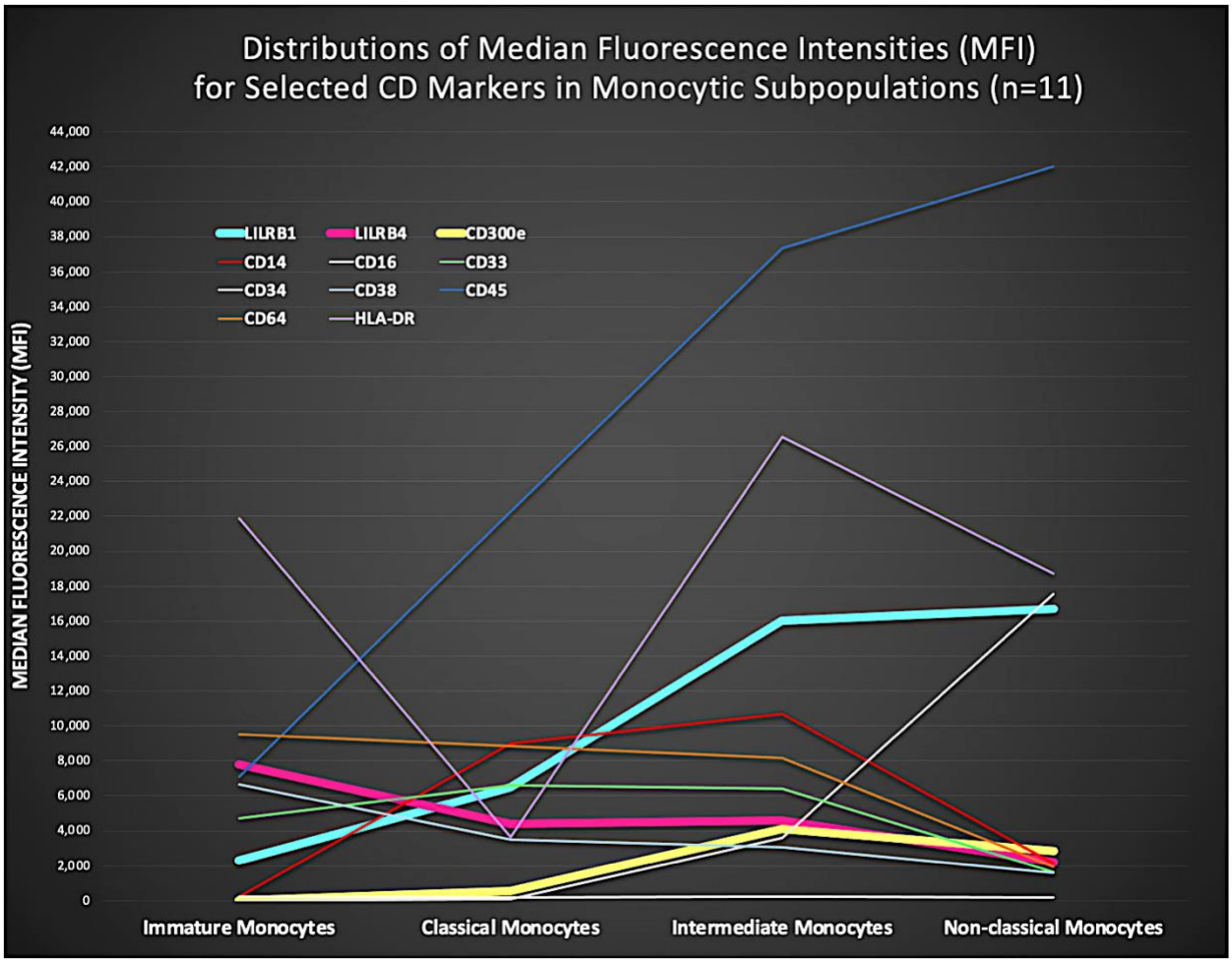


**Figure 2: Distributions of median fluorescence intensities (MFI) for selected CD markers in monocytic subpopulations in normal control samples.** A comprehensive view of immunophenotypic characteristics of the 11 antigenic markers incorporated in the monocytic assay

utilizing normal control samples (n=11) show dynamic immunophenotypic expressions among immature, classical, intermediate, and non-classical monocytic populations.

**Normal immature monocytic cells co-express LILRB1 and LILRB4**

Similar to the previous studies, our findings consistently show that immature monocytic cells co-expressed LILRB1 and LILRB4 with moderate to bright intensity, respectively (**Figure 3)**.[11] The expression of CD300e was absent in CD14 negative immature monocytic cells; however, as the CD14 reaches its peak level during the maturation process, the expression of CD300e emerges in mature monocytic cells. These findings support previous research indicating that CD300e serves as a marker for mature monocytic cells (**Figure 3-A,e**).[4] Further assessment of selected myelomonocytic markers demonstrated a spectrum of expression in immature monocytes, including dim to absent CD14, bright CD33, bright CD38, moderate CD45, bright CD64, and bright HLA-DR without CD16 or CD34 **(Figures 2 and 3)**. Of note, a small subset of normal BM control cases showed dim positive CD34 expression in immature monocytic cells with dim LILRB1 and LILRB4 expression (data not shown). Furthermore, the level of CD38 intensity observed in immature monocytic cells was comparatively lower than that of plasma cells but slightly higher than the background myeloid populations (data not shown).

**Normal mature monocytes co-express LILRB1, LILRB4, and CD300e**

Mature monocytes in normal control samples showed co-expression of LILRB1 and LILRB4, with prominent CD300e expression **(Figures 2 and 3)**. Notably, the expression of novel markers exhibited distinct intensity level shifts in mature monocytes compared to their immature counterparts, characterized by increased LILRB1, decreased LILRB4, and heterogeneous to

moderate CD300e expression **(Figures 2 and 3-A)**. As highlighted in previous section, CD300e is exclusively expressed in mature monocytes, establishing it as a reliable marker in conjunction with CD14 for maturity assessment. Additional antigenic expression of mature monocytes included moderate to bright CD14, variable CD16, bright CD33, CD38, bright CD45, bright CD64, and HLA-DR without CD34 **(Figures 2 and 3)**.

**A.**

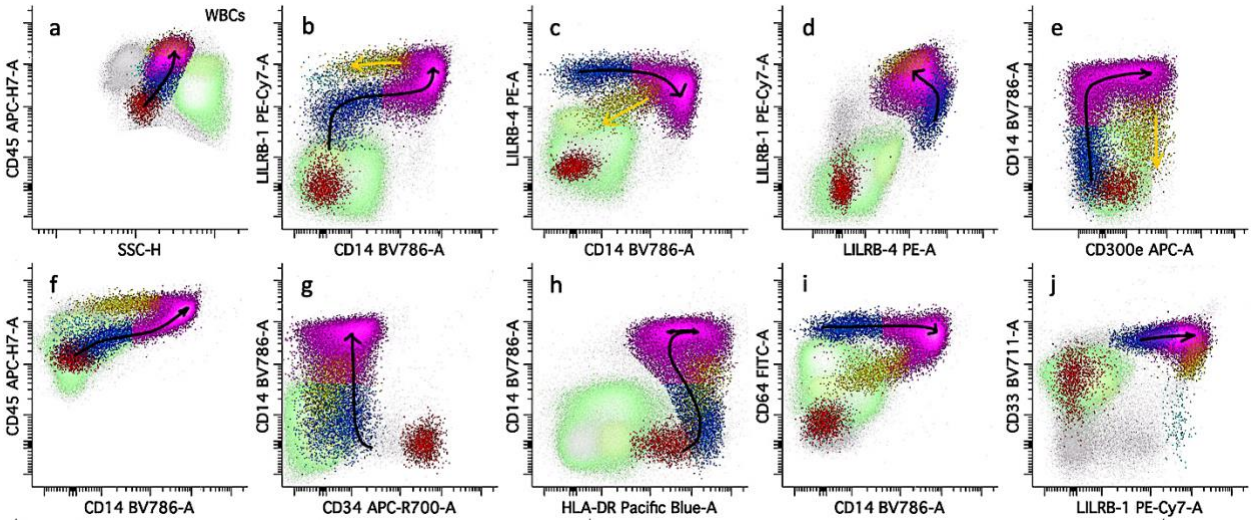


**B.**

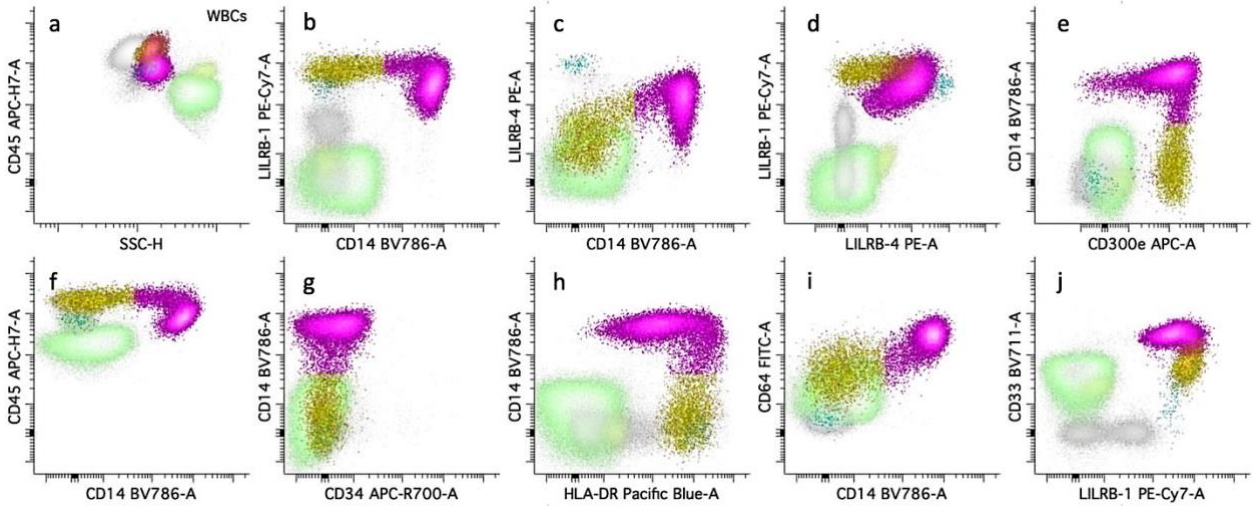


**Figure 3**: **LILRB1, LILRB4, and CD300e expression in monocytes comparison to other white blood cell populations in normal bone marrow (BM) and peripheral blood (PB) samples.**

**A. Normal BM:** Monocytes display a comparatively dimmer CD45 expression in their immature state, which progressively increases as they mature **(A. a)**. Monocytes are characterized by the co-expression of LILRB1 and LILRB4, along with CD300e expression as CD14 intensity reaches its peak, indicating full monocytic maturation **(A. b-e)**. Immature monocytes express dim to moderate LILRB1, moderate LILRB4 without CD14 and CD300e (dark blue). As maturation progresses, an inverse trend in LILRB1 and LILRB4 intensities can be observed, highlighting the differentiation from immature to mature monocytic stages. Distinctively, non-classical monocytes exhibit brightest LILRB1 intensity and variably dim LILRB4 expression with uniformly bright CD300e expression. Plasmacytoid dendritic cells (pDCs) demonstrate moderate to bright co-expression of LILRB1 and LILRB4 but lack CD14, CD64, and CD300e, rendering these cells readily distinguishable from monocytic cells. Eosinophils express LILRB1 at a dim level without LILRB4, further differentiated by bright side scatter (SSC) property and absence of CD14, CD64. Lymphocyte subset expresses LILRB1 intensity level similar to the immature monocytic cells and differentiated by absence of myelomonocytic markers. **B. Normal PB**: PB contains primarily mature monocytic and other hematopoietic cells with immunophenotypic patterns similar to those found in BM samples. **Color code**: dark blue (immature monocytes), magenta (maturing/ mature monocytes), yellow (non-classical monocytes), red (myeloblasts), green (granulocytes), light green (eosinophils), cyan (pDCs), and gray (lymphocytes).

**A detailed analysis of mature monocytic subsets reveals distinct immunophenotypic features between classical, intermediate, and non-classical monocytes**

Additionally, we conducted a detailed MFC assessment of classical, intermediate, and non-classical monocytes to provide precise immunophenotypic signatures beyond CD14 and CD16

among these mature monocytic subsets. Classical monocytes (magenta; $CD14^{++}/CD16^{-}$) expressed bright CD33, CD38, moderate CD45, CD64, heterogeneous CD300e, moderate to heterogeneous HLA-DR, moderate to bright LILRB1 and LILRB4 **(Figure 4 and 5)**. Intermediate monocytes (blue; $CD14^{+}/CD16^{+}$) were immediately recognized by bright CD45 expression with a dimmer SSC intensity with bright CD33, moderate to bright CD38, slightly decreased CD64, HLA-DR, bright LILRB1, and moderate LILRB4 **(figure 4)**. Non-classical monocytes (orange; $CD14^{dim/-}/CD16^{++}$) also exhibited similar CD45 and SSC expression as intermediate monocytes and express moderate CD33, dim CD38, dim CD64, uniformly bright CD300e, bright HLA-DR, bright LILRB1, and variably dim LILRB4 **(figure 4)**. Consistent with prior research, our study observed that non-classical monocytes display notably bright and uniform LILRB1 expression compared to other monocytic subsets. **(Figures 3-A,b; B,b, and 4-c)**.[11]

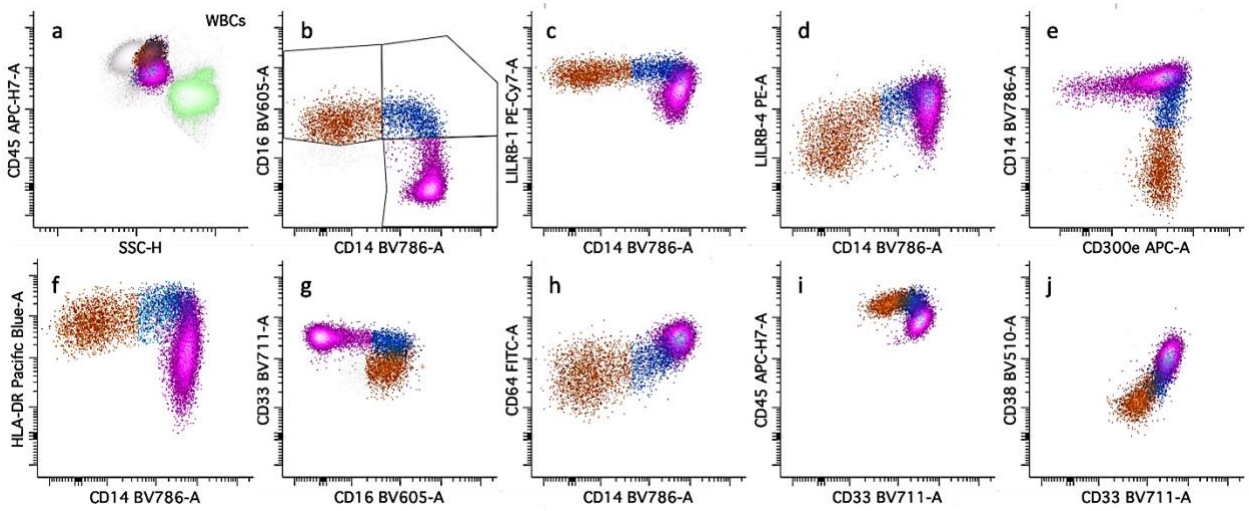


**Figure 4: Immunophenotypic features of classical, intermediate, and non-classical monocytes in normal peripheral blood (PB).** Plot **(a)** highlights and contrasts mature monocytic subsets against other white blood cell populations expressing moderate to bright CD45 and intermediate side scatter expression. Plots **(b-j)** show monocytic subsets against various marker combinations, highlighting unique features within each population. Classical monocytes (magenta)

are characterized by moderate to bright CD14 without CD16 and express bright CD33, CD38, CD45, and CD64, heterogeneous CD300e, moderate to heterogeneous HLA-DR, bright LILRB1, and moderate LILRB4. Intermediate monocytes (blue) are identified by moderate expression of CD14 and CD16 and differentiated by increased CD45 and slightly decreased SSC properties with bright CD33, moderate CD38, CD300e, bright HLA-DR, LILRB1, and LILRB4 with slightly decreased CD64 expression. Non-classical monocytes (orange) are defined by dim to absent CD14 and high CD16 expressions with brightest CD45 and dim SSC properties. Additional distinguishing features of non-classical monocytes include decreased CD33, dim CD38, dim CD64, bright HLA-DR, bright LILRB1, dim variable LILRB4, and bright CD300e expressions. **Color code:** magenta (classical monocytes), blue (intermediate monocytes), and orange (non-classical monocytes), green (myelocytic cells), and gray (lymphocytic cells).

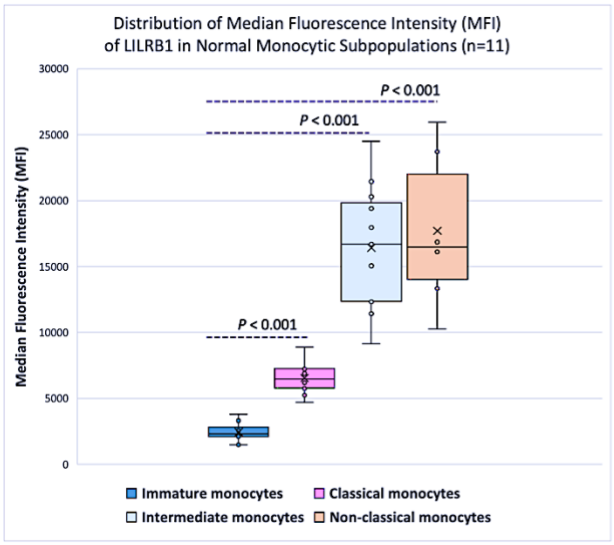


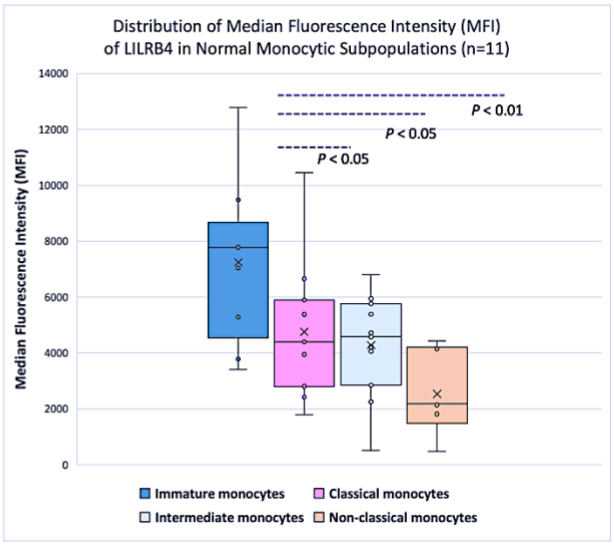


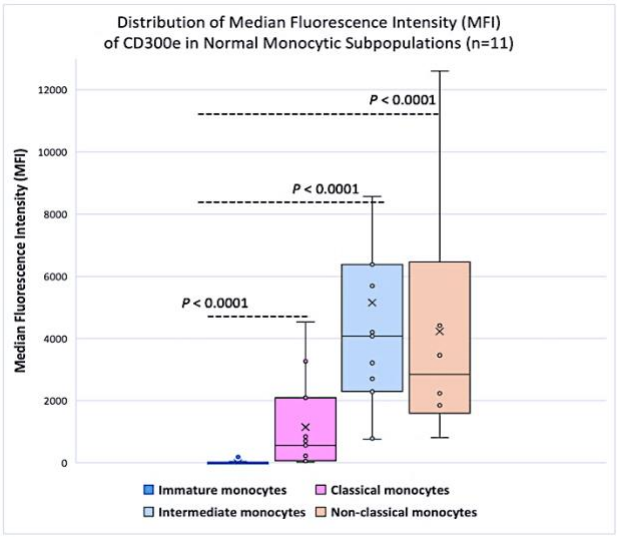


**Figure 5. Box-and-whisker plots demonstrating distribution of median fluorescence intensity (MFI) of LILRB1, LILRB4, and CD300e in immature, classical, intermediate, and non-classical monocytes (n=11).** Box and whisker plots highlight the differences in novel marker expression between immature monocytes and the mature subsets - classical, intermediate, and non-classical monocytes. These data demonstrate the specificity and sensitivity provided by novel markers, LILRB1, LILRB4, and CD300e, in monocytic subset evaluation. MFI values were quantitatively evaluated using the Mann-Whitney U test and *P*-values less than 0.05 were considered significant.

**Immunophenotypic features of monocytes in reactive monocytosis**

Reactive monocytosis controls (n=10, BM=7, PB=3) exhibited an increase in the proportion of total monocytic population (median 13.2%, range 10.0% - 33.9% total WBCs) and the reactive subsets (data not shown) compared to the normal control cases (n=11, BM=9, PB=2; median 6.8%, range 3.8% - 8.7% of total WBCs). Overall, the antigenic expression patterns and intensities in reactive monocytes were similar to those observed in normal controls.

**LILRB1, LILRB4 and CD300e expression profiling in other hematopoietic cell populations**

Our study extended the assessment of LILRB1, LILRB4, and CD300e expression to other hematopoietic cell populations in normal PB and BM controls. We observed varying levels of LILRB1 and LILRB4 expression in pDCs, eosinophils, lymphocyte subset, and plasma cell; nevertheless, they were readily distinguishable from monocytic cells by their unique antigenic features (**Figure 3**). Additionally, CD300e expression was not observed in these WBC populations. In line with previous findings, pDCs expressed moderate to bright LILRB1 and LILRB4, similar to those in monocytic cells **(Figure 3. A-j; B-b,c,d,j)**.[11] However, pDCs were readily distinguishable from monocytic cells as they do not express CD14 and CD64. Eosinophils exabit relatively dim LILRB4 without LILRB1 or CD300e expression and further distinguished by their bright SSC and CD45 properties **(Figure 3)**. A subset of lymphocytes (gray) and plasma cells (not shown) also expressed LILRB1 at a dim intensity comparable to that of immature monocytes but were consistently negative for both LILRB4 and CD300e expression and was further distinguished by absence of myelomonocytic marker expression **(Figure 3)**.

**Novel markers LILRB1, LILRB4, and CD300e facilitate distinction between M-AML and other AML subtypes**

In line with previous findings, all neoplastic cases in our study demonstrated co-expression of LILRB1 and LILRB4 in monocytic cells across all maturational stages, highlighted with yellow box in **Figure 6**.[11] M-AML control cases predominantly showed marked monocytosis (median 53.1%, range 7.4% - 98.3 % total WBCs), including notably expanded immature monocytic populations (median 21.7%, range 0.8% - 98.0% total WBCs). These immature monocytic cells typically exhibit dim to absent CD14, bright CD33, intermediate to dim CD45, moderate to bright CD64, bright HLA-DR, LILRB1, and LILRB4 without CD34 or CD300e expression in similar fashion observe in normal control cases. Myeloid blasts and granulocytic populations did not exhibit any discernable levels of LILRB1, LILRB4, or CD300e across all leukemia cases evaluated. To enhance these qualitative observations with quantitative evidence, we performed a comparative analysis of MFI for LILRB1 and LILRB4, identifying statistically significant differences between immature monocytic cells and myeloblasts across M-AML, CMML, and AML cases (**Figure 7**; monoblasts versus myeloblasts : M-AML $p < 0.001$; CMML $p < 0.05$; AML $p < 0.001$ for both LILRB1/4). Furthermore, CD300e expression was exclusive to mature monocytes and absent in myeloblasts and granulocytic cells across all leukemic control cases similar to the findings in normal control samples (**Figure 6**). Our comprehensive findings support previous studies and underscore the diagnostic significance of LILRB1, LILRB4, and CD300e for defining monocytic lineage in neoplastic cases. Of note, APL and BPDCN control cases were excluded from the statistical assessments due to markedly small monocytic populations and limited sample size.

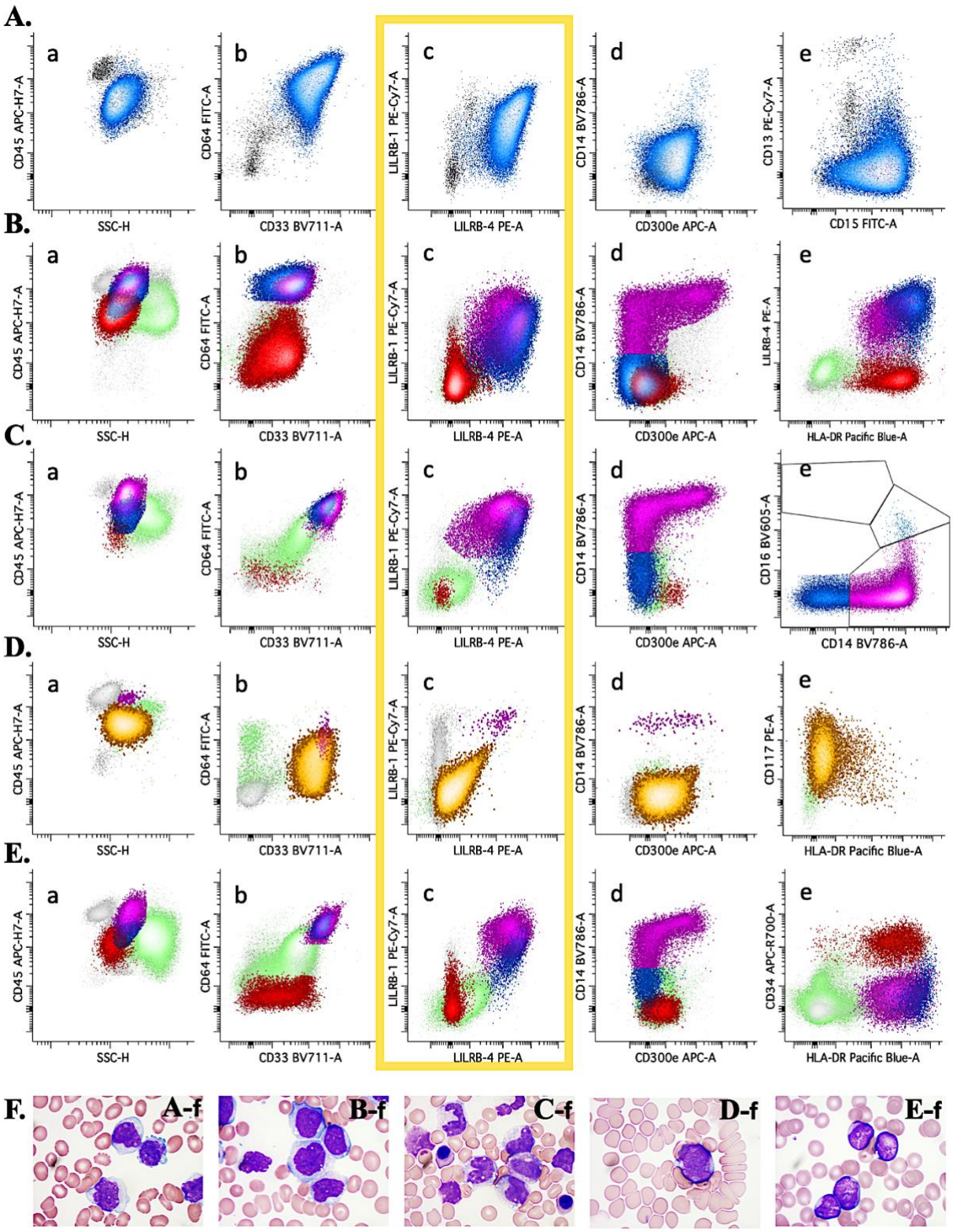


**Figure 6: Comparisons of expression patterns of LILRB1, LILRB4, and CD300e in M-AML versus other AML subsets.**

**Figure 6: Row A**. **Acute monocytic leukemia (BM):** Expanded abnormal monoblasts population (blue) with dim/negative CD13, absent CD14, moderate to bright CD15, and dim CD45 expression suggesting its immature nature. The co-expression of LILRB1 and LILRB4 without CD300e, together with moderate to bright CD33 and CD64 suggests an early monocytic lineage commitment of the blast population, consistent with morphologic findings (Row F. A-f) **Row B**. **Acute myelomonocytic leukemia (BM):** An expansion of leukemic monocytic cells and myeloblasts characterizes this case. The CD45 versus SSC plot highlights the differentiation between CD14-negative immature monocytes (blue) with intermediate to moderate CD45 expression, and the maturing/mature monocytes (magenta) with moderate to bright CD45, from the myeloblasts (red) exhibiting dim CD45 expression (B-a). Both immature and mature monocytic populations are distinguished by the co-expression of LILRB1 and 4 with bright CD64. In contrast, CD34 absent (not shown) abnormal myeloblasts are negative for LILRB1/4 with dim to negative CD64. Notably, both monocytic and myeloblastic populations exhibit abnormally low level of CD33 expression in this high-grade myeloid neoplasm case (B-b). **Row C. Chronic myelomonocytic leukemia (BM):** This relapsed CMML case features increased proportion of monocytes (32.7% total WBCs) with abnormal myeloblast population. A clear separation between immature (6.0% total WBCs; blue) and mature (magenta) monocytes from myeloblasts (red) and granulocytic populations (green) is evident in the LILRB1 vs. LILRB4 plot (C-c) and the plot C-e suggesting a dominance of classical monocytes ( $CD14^{++}/CD16^{-}$, 24.0% total WBCs; 77.0% total monocytes), reflecting the disease's characteristic monocyte subset distribution. **Row D. Acute promyelocytic leukemia (PB):** Abnormal promyelocytes (yellow) identified by predominantly absent CD34, variable CD117 (not shown), moderate to bright CD33, dim CD64, with absent LILRB1, LILRB4, and CD300e expression. In contrast, a small fraction of monocytic population

(magenta) can be appreciated by the co-expression of LILRB1, LILRB4, and CD300e, highlighting the sensitivity and specificity of these novel markers. **Row E** represents AML case with expanded myeloblast population (red). Across all observed leukemia cases, myeloblasts consistently lack discernible expressions of LILRB1, LILRB4, or CD300e, whereas monocytic populations continue to co-express these novel markers. **Row F:** Morphological correlates at 100x magnification cases from A-E. **Color code**: dark blue (monoblasts/ promonocytes), magenta (maturing/ mature monocytes), green (granulocytes), yellow (promyelocytes), red (myeloblasts), and gray (lymphocytes).

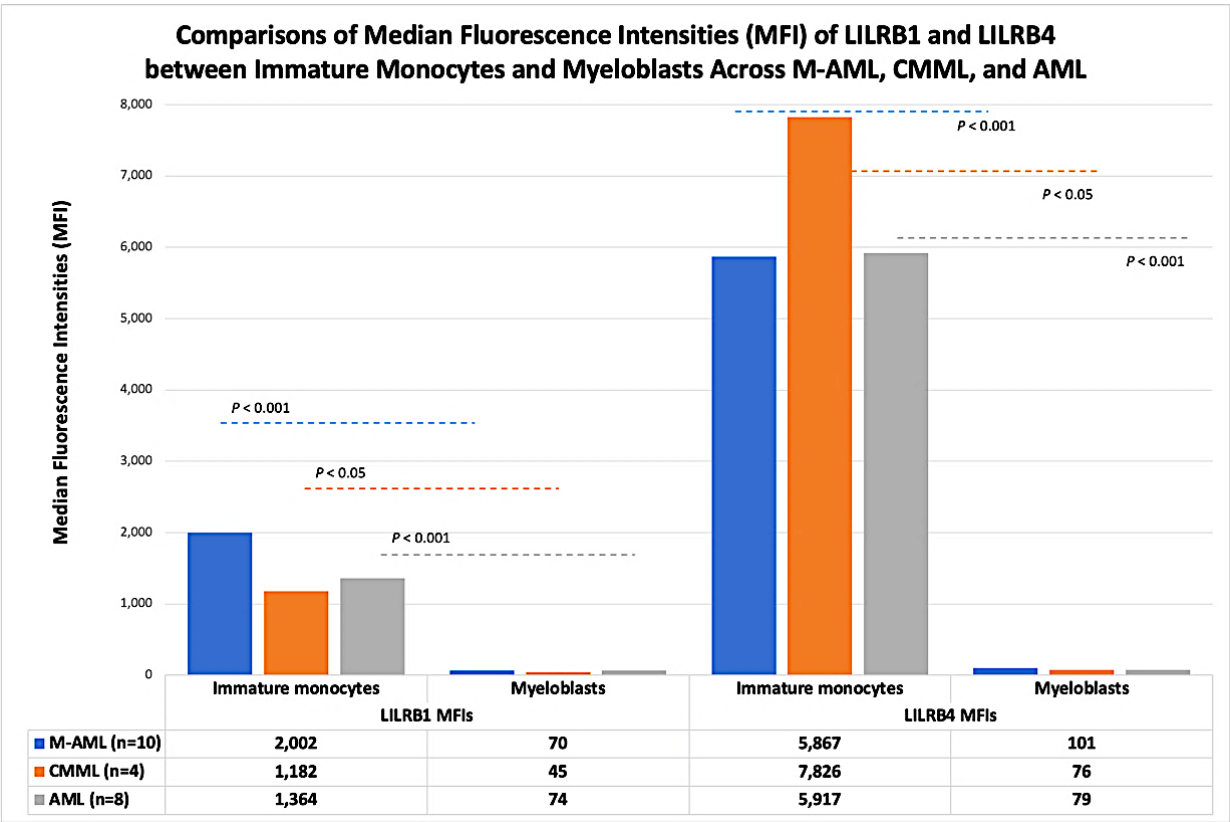


**Figure 7: Comparisons of median fluorescence intensities (MFI) of LILRB1 and LILRB4 between immature monocytes and myeloblasts across M-AML, CMML, and AML.** A comparison study of MFI values for LILRB1 and LILRB4 expression between immature monocytes and myeloblasts in M-AML, CMML, and AML revealed statistically significant *p*-values. MFI values were quantitatively evaluated using the Mann-Whitney U test and *P*-values less than 0.05 were considered significant. **Abbreviation:** M-AML (acute myeloid leukemia with monocytic differentiation), CMML (chronic myelomonocytic leukemia), and AML (acute myeloid leukemia).

### 3.2. Immunophenotypic characteristics of normal, CD56+ reactive, and CD56+ neoplastic plasmacytoid dendritic cells (pDCs)

This section elucidates the immunophenotypic profiles of pDCs in their normal, reactive, and neoplastic states, which is a crucial aspect for the accurate classification and post-therapeutic monitoring of BPDCN. Comprehensive immunophenotypic profiling of pDCs was conducted by assessing 12 antigenic markers included in the optimized pDC assay: CD2, CD4, CD7, CD34, CD38, CD45, CD56, CD64, CD123, CD303, CD304, and HLA-DR (**Figure 8**).

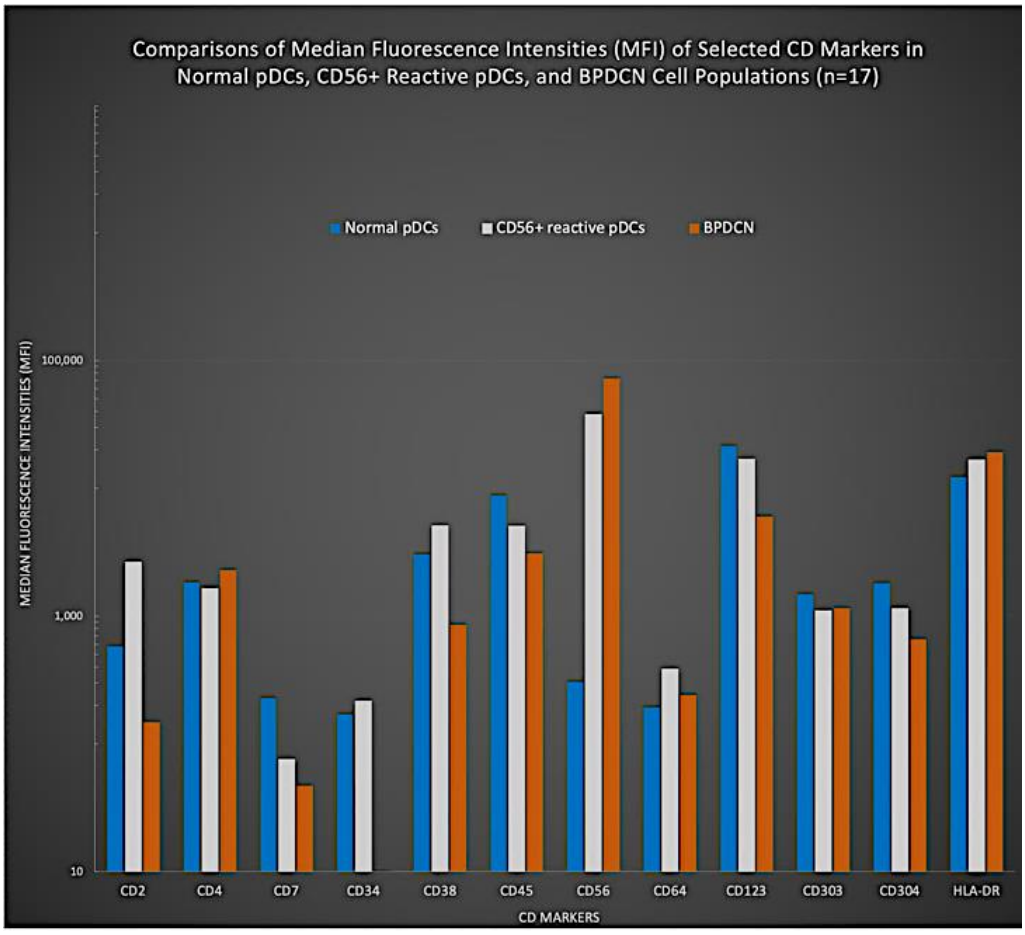


**Figure 8. Comparisons of median fluorescence intensities (MFI) of selected CD markers in normal, CD56+ reactive, and BPDCN cell populations.** The immunophenotypic characteristics of the 12 antigenic markers incorporated in the pDC assay showcasing dynamic immunophenotypic expressions of normal, CD56+ reactive, and BPDCN pDCs.

**Normal pDCs co-express CD303 and CD304 and show distinct CD2 and CD7 expression**

In normal control cases, pDCs constituted a median of 0.37% of total WBCs (n=17, BM=15, PB=2, range 0.02% - 3.2%). Normal pDCs typically reside within the blast gate expressing slightly higher CD45 intensity relative to myeloblasts (**Figure 9,** blast gate and myeloblasts are not highlighted). Normal pDCs were further characterized by CD4, moderate CD38, bright CD123, and moderate to bright HLA-DR without CD34, CD56, or CD64 expression. Additionally, co-expression of the novel pDC-markers CD303 and CD304 at a moderate intensity was observed in all normal control samples similar to the previous studies **(Figure 9)**.[7,19] In line with Wang et al., one of the notable findings was bimodal expression of CD2 and presence of small CD7 positive pDC subsets seen in all normal samples.[19] These subsets maintained the typical pDC antigenic marker expression as described above (**Figure 9. A-h,j; B-h,j** ). This finding further supports the complex and heterogeneous nature of pDCs, underscoring their unique immunophenotypic profile within the pDC population.

**CD56+ reactive pDCs consistently exhibited distinct immunophenotypic pattern different from normal counterparts**

CD56+ reactive pDCs were observed in a subset of the normal BM control cases (5 out of 12), accounting for a small percentage of total pDCs (median 16.8%, range 1.5% - 27.6% of total pDCs). Consistent with previous findings, these reactive CD56+ pDCs exhibited a distinctive immunophenotypic profile, characterized by positive CD2, negative CD7 with uniformly bright CD38 expression **(Figure 9-c)**.[19] Other marker expressions in CD56+ reactive pDCs were similar to that observed on normal counterparts **(Figure 9)**.

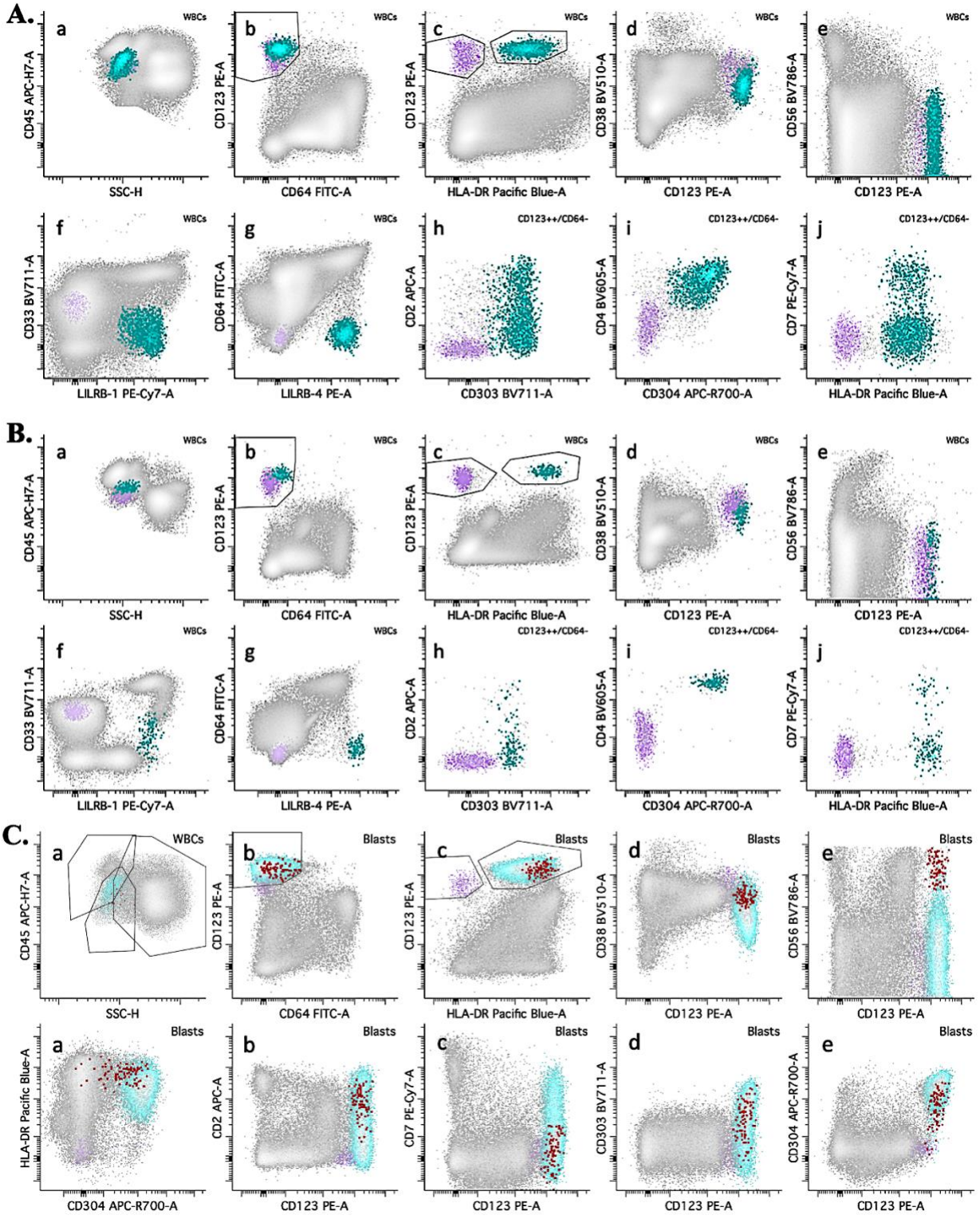


**Figure 9: Immunophenotypic characteristics of normal and CD56+ reactive plasmacytoid dendritic cells (pDCs) in normal bone marrow (BM) and peripheral (PB) cases.** Row A (BM)

and B (PB) showcase typical immunophenotype of pDCs (light blue) and row C (BM) represent a case including both normal (cyan) and CD56+ reactive pDC subsets (red). Typically, pDCs express intermediate to dim CD45 expression, which reside within the CD45 vs SSC define blast gate ( gating not depicted in the figure). The gating strategy for pDCs initiated by identifying cells that displays bright CD123 without CD64 and further delineated based on positive HLA-DR expression (A and B, a-c). Normal pDCs consistently positive for CD4, CD38, CD303, and CD304. A bimodal CD2 expression and a small subset of CD7 are consistently observed in pDCs in all normal cases (A and B, h and j). Additionally, pDCs co-expresse LILRB-1 and LILRB4 on at a similar intensity seen in monocytes (A and B. f,g). It is noteworthy that CD33 intensity in pDCs was consistently lower than that of monocytic population. **Row C**: A BPDCN post-therapy case with approximately 3% normal plasmacytoid dendritic cells (cyan) with approximately 1% CD56+ reactive sub population (red). The small reactive pDC population can be appreciated with its distinctive immunophenotypic expression of positive CD2, negative CD7, and uniformly bright CD38 expression, distinguishing it from the normal pDC population. **Color code**: cyan (pDCs in row C), red (reactive CD56+ pDCs), purple (basophils), gray (other hematopoietic cells).

**Immunophenotypic Characteristics of CD56+ BPDCN Cells**

CD56+ BPDCN cells display a distinct immunophenotypic feature that is noticeably deviates from that of both normal and CD56+ reactive pDCs. BPDCN cells showed decreased CD45 expression with intensity levels ranging from dim to absent in our cohort (**Figure 10**). These neoplastic pDCs predominantly expressed CD4, decreased CD38 and decreased CD123 compared to their normal and CD56+ reactive counterparts (**Figure 10; Table 5**, normal pDC vs. BPDCN $p < 0.001$ for both CD38 and CD123; CD56+ reactive pDCs vs. BPDCN $p < 0.001$ and $p < 0.05$ for CD38 and CD123, respectively ). HLA-DR expression was typically increased, while CD303 and CD304 expression were variably decreased, with the absence of CD64. It is worth noting that there was a significant difference in MFI values for CD304 between normal pDCs and CD56+ neoplastic pDCs (**Table 5,** $p < 0.05$). However, there was no statistical significance between CD56+ reactive and CD56+ neoplastic pDCs ($p = 0.1$). Additionally, we observed variable expression of CD2 and CD7 on CD56+ neoplastic cells similar to the previous studies (**Figure 10 A and B**).[19] Among the 10 BPDCN control cases (BM=8, PB=2), 6 cases (BM=4, PB=2) exhibited CD2-/CD7+ expression, while the other 4 BM cases displayed CD2+/CD7- on neoplastic pDCs. This unique immunophenotypic heterogeneity within our BPDCN cohort contrasts with the consistent CD2+/CD7- profile observed in reactive CD56+ pDC control cases (**Figure 9-C, 10 and 11-C)**.

**Table 5: Comparisons of median fluorescence intensities (MFI) of 12 antigens in pDC assay between normal, CD56+ reactive, and BPDCN cells**

| | MFI (Mean Fluorescence Intensity) | | | *p*-value | |
|---|---|---|---|---|---|
| | Normal pDCs | CD56+ reactive pDCs | BPDCN | Normal pDCs vs. BPDCN | CD56+ reactive pDCs vs. BPDCN |
| **CD2** | 581 | 2,658 | 148 | 0.127 | 0.129 |
| **CD4** | 1,841 | 1,612 | 2,295 | 0.639 | 0.606 |
| **CD7** | 229 | 76 | 47 | 0.066 | 0.859 |
| **CD34** | 170 | 217 | 8 | **<0.001** | **<0.05** |
| **CD38** | 3,041 | 5,125 | 855 | **<0.001** | **<0.001** |
| **CD45** | 8,774 | 5,089 | 3,103 | **<0.001** | 0.099 |
| **CD56** | 254 | 38,201 | 72,529 | **<0.0001** | 0.679 |
| **CD64** | 219 | 385 | 241 | 0.05 | 0.147 |
| **CD123** | 21,933 | 17,023 | 6,019 | **<0.0001** | **<0.05** |
| **CD303** | 1,506 | 1,108 | 1,154 | 0.148 | 0.797 |
| **CD304** | 1,944 | 1,151 | 661 | **<0.05** | 0.112 |
| **HLA-DR** | 7,993 | 16,790 | 19,161 | 0.115 | 0.953 |

MFI values were quantitatively evaluated using the Mann-Whitney U test and *P*-values less than 0.05 were considered significant. **Abbreviations**: pDCs (plasmacytoid dendritic cells), BPDCN (blastic plasmacytoid dendritic cell neoplasm).

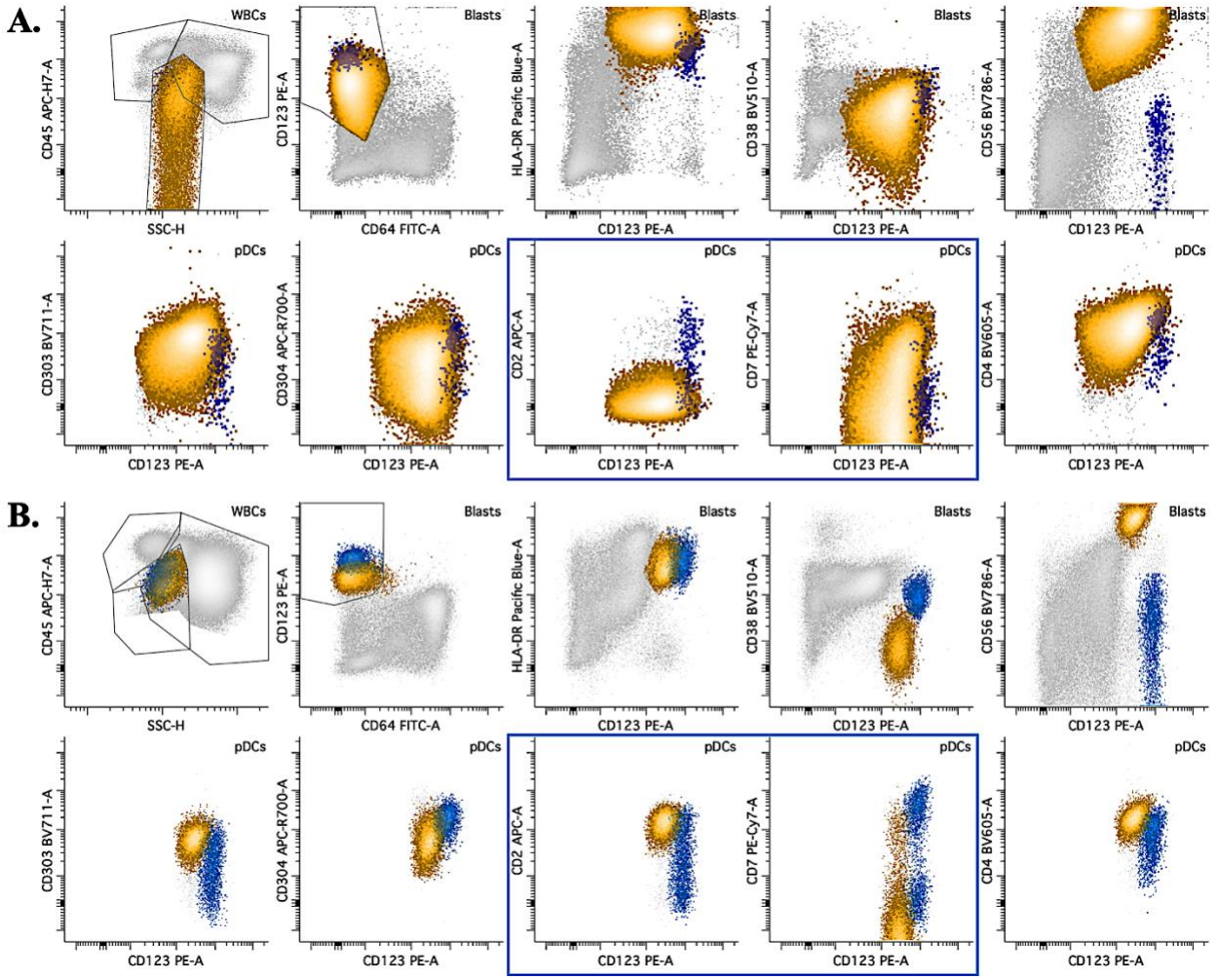


**Figure 10: A representative BPDCN cases in bone marrow sample highlighting CD56+ BPDCN cells and normal pDCs.** BPDCN example Panel A and B illustrate the flow cytometric analysis data from BM samples, demonstrating the distinct antigenic profiles of BPDCN and normal pDCs. Both examples showcase CD56+ neoplastic cells (yellow) with notably diminished CD45 expression comparison to the normal counterpart (dark blue), ranging from dim to absent. BPDCN cells predominantly express CD4 with decreased CD38 and CD123. Expression of CD303 and CD304 show variable expression from dim to bright. As depicted in blue box, the BPDCN cells in our cohort showed a unique immunophenotypic pattern between CD2 and CD7, with some cases showing a CD2-/CD7+ profile (A), while others exhibit CD2+/CD7- expression (B). **Color**

**code:** yellow (BPDCN cells), blue/ dark blue (normal CD56- pDCs), and gray (other hematopoietic cells).

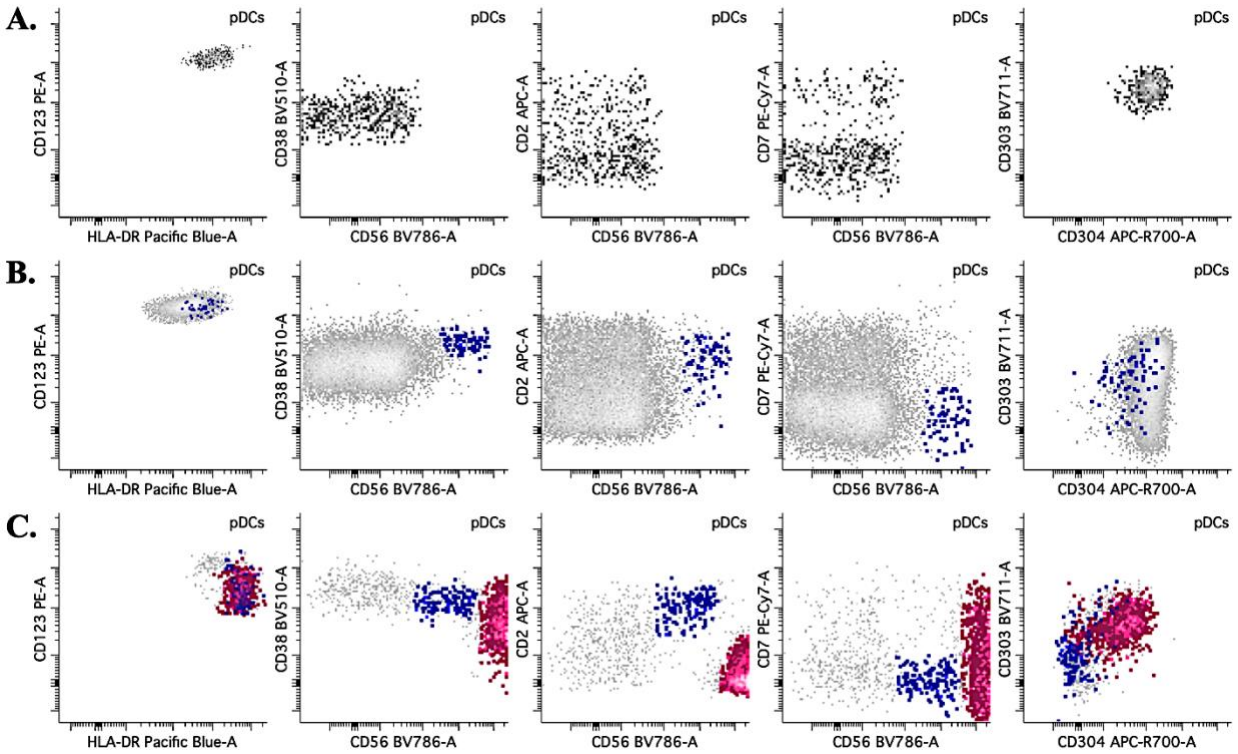


**Figure 11: Comparative Immunophenotypic Profiles of Normal pDCs, CD56+ Reactive pDCs, and BPDCN Cells.** **Row A** presents normal pDCs (gray), expressing characteristic markers expressing CD2 with bimodal pattern, CD7 in small subset, moderate CD38, bright CD123, CD303, CD304 and HLA-DR. **In row B**, the data illustrate a case presented with both normal and CD56+ reactive pDCs, with reactive pDCs showing positive CD2, negative CD7, and uniformly increased CD38 with variable CD303 and CD304 expression. **Row C** includes a case containing all three pDC populations: normal pDCs, CD56+ reactive pDCs, and BPDCN cells. BPDCN cells display antigenic expression profiles that are markedly different from both normal and reactive CD56+ pDCs, characterized by variably decreased CD38 and CD123. Co-expression

of CD303 and CD304 is apparent in neoplastic cells with slight decreased in intensity, with CD2 and CD7 expression also being distinctly different from that observed in CD56+ reactive pDCs.

**Color code:** Red (BPDCN cells), dark blue (reactive CD56+ pDCs), and gray (CD56- normal pDCs)

## 4. Discussion

Advancements in medical technology and the discovery of novel markers have significantly improved the capabilities of MFC in the classification and diagnosis of hematological neoplasms. One of the persistent challenges in diagnostic hematopathology is accurately determining the maturation stages and defining aberrancy within monocytic and plasmacytoid dendritic cell lineages.[11,19] These complexities underscore the need for refined assessment tools capable of discerning the subtle phenotypic nuances of these distinct cell populations.

In response to this challenge, the primary objective of our study was to design and optimize MFC assays for the comprehensive assessment of monocytic cells and pDCs. Our aim was to bridge the diagnostic gaps by utilizing these optimized assays to provide enhanced sensitivity and specificity, with a particular focus on monocytic leukemia and BPDCN. Our findings demonstrate that optimized assays offer enhanced detection and characterization capabilities compared to the current methods. The following sections will discuss these elements in detail, laying the foundation for an understanding of impact of this validation study on the field of hematopathology.

**Monocytic assay optimization:**

One of the primary challenges in assessing monocytic populations is the accurate delineation of maturational stages and the effective differentiation between reactive monocytic subsets and other closely related lineage populations. These include myeloid blasts, various myeloid cells, including those with dysplastic features, and dendritic cell populations, all of which exhibit overlapping antigen expressions. In this study, we addressed this complexity by integrating novel markers LILRB1, LILRB4, and CD300e with established myelomonocytic markers, resulting in a significant improvement in specificity. This enhancement enabled a more precise distinction between monocytes at different stages of maturation within a heterogeneous cell population (**Figures 2, 3 and 5**).

**Utility of the optimized monocytic assay in delineating immature monocytic cells**

The optimized monocytic assay demonstrated the capacity for precise discrimination between immature monocytic cells and their mature counterparts, as well as other hematopoietic lineages. Immature monocytic cells are initially characterized by the immunophenotype CD14-/CD33+/CD64++/HLA-DR++, followed by co-expression of LILRB1 and LILRB4 with the absence of CD300e, providing a unique immunophenotypic signature (**Figure 2 and 3**). It is important to note that the distinct features that segregate CD14-/CD300e- from $CD14^{dim/+}$/CD300e- immature monocytes remain elusive and present a potential area for future research. We recommend further investigation, possibly through sorting experiments, to ascertain whether there are discernible morphological differences between these two subpopulations. Such studies could illuminate the pathophysiological significance of these subsets and further refine the performance of the assay.

**Immunophenotypic characterization of mature monocytic subsets:**

As monocytic cells mature and differentiate, there is a notable upregulation in CD14, CD300e, and LILRB1, with a slight downregulation of LILRB4 (**Figure 3**). In addition to assessing monocyte maturation, the optimized monocytic assay with the new makers facilitates the improved delineation of mature monocytic subsets: classical (CD14++/CD16-), intermediate (CD14+/CD16+), and non-classical monocytes ($CD14^{dim/-}$/CD16++). **Figures 4** depicts how mature monocytic subsets can be clearly distinguished by their unique antigenic profiles provided by the combinations of markers utilized in the optimized 11-color monocytic assay. Non-classical monocytes, in particular, often express brightest LILRB1 intensity, consistent with findings from a previous study (**Figure 3 and 4**).[11] Box and whisker plots in **Figure 5** present a clear distinctions of novel markers, LILRB1, LILRB4, and CD300e, between immature and each mature monocyte subsets. Each new markers coupled with useful myelomonocytic markers provide distinct profiles for each monocytic subset, facilitating precise identification and classification. Detailed immunophenotypic profiling capacity provided by the optimized monocytic assay is crucial for elucidating the heterogeneity within the monocyte pool. Further studies are recommended to correlate current findings with specific disease characteristics and monitor post-therapy responses.

**Enhanced precision and reliability of the monocytic assay for specifically identifying cells of monocytic lineage in challenging cases**

Myeloid cells may exhibit increased expression of antigens typically associated with monocytic lineage assignment, such as CD14 and CD64, during reactive states or disease processes.[12] This expression can obscure the distinction between myeloid and monocytic populations, making precise identification challenging. The assay's enhanced precision is demonstrated in **Figures 3**

**and 5**, where monocytes are clearly distinguished by their co-expression of LILRB1 and LILRB4 in all stages of maturation, while myeloblasts and myeloid cells consistently lack these markers, validating the specificity and reliability of the monocytic assay under both normal and neoplastic conditions.

A peripheral blood (PB) control case featuring CD64-negative monocytes otherwise featuring typical mature monocytic immunophenotype and morphology provided an excellent opportunity to validate the assay's diagnostic capabilities. The monocytic assay reliably confirmed these cells as monocytic lineage based on the co-expression of LILRB1, LILRB4, and strong CD300e, immunophenotype indicative of mature monocytes (data not provided). Although rare, this example validated the diagnostic confidence provided by the inclusion of the novel markers.

**Implications for classification and diagnosis of monocytic neoplasms**

The incorporation of LILRB1, LILRB4, and CD300e into the monocytic assay provided substantial improvement in the evaluation of hematopoietic neoplasms, enhancing both classification and diagnostic precision. This section will explore how these markers perform within the context of neoplastic conditions and their potential impact on treatment strategies.

Consistent with prior research, our validation study in differential findings in neoplastic cases reveal that monocytic cells persistently co-express LILRB1, LILRB4, and CD300e, following similar maturational patterns observed in normal control cases (**Figure 6**).[4,11,19] Notably, the majority of M-AML cases qualitatively demonstrated a downregulation in LILRB1 and an upregulation in LILRB4 compared to normal cases. However, due to the limited sample size and

a lack of statistical significance ($p > 0.05$), these findings should be considered preliminary and further investigation with larger sample size is necessary to support these observation.

Deng et al.[21] highlighted the significance of LILRB4 in modulating leukemic cell infiltration pathways and T cell suppression in M-AML, suggesting its utility beyond differential diagnosis and pointing towards therapeutic potential. This is corroborated by recent preclinical trials which have shown promise in LILRB4-targeted CAR-T therapy, effectively targeting leukemic cells while sparing normal hematopoietic precursors.[22]

**pDC assay optimization:**

Development and optimization of the pDC assay was motivated by the need for an effective tool that is capable of distinguishing between normal, CD56+ reactive, and CD56+ neoplastic pDCs in the context of BPDCN. This optimization was driven by the complex immunophenotypic nuances that exist between CD56+ reactive pDCs and their neoplastic counterparts, which often complicate accurate diagnosis and monitoring. In line with previous studies, the adoption of novel markers such as CD303 and CD304, along with CD2 and CD7, shown improved diagnostic capability of the assay to percisly identify and categorize different pDC subpopulations.[19]

**Immunophenotypic distinction between normal and CD56+ reactive pDCs**

A comprehensive immunophenotyping between the normal pDCs and reactive CD56+ pDCs revealed consistent antigenic patterns that facilitate their differentiation. Both normal and reactive populations typically fall within the CD45 versus SSC blast gate, characterized by their intermediate to dim CD45 expression levels. Normal pDCs exhibit a defined immunophenotype:

bimodal CD2 expression, CD4, a small subset expressing CD7, moderate CD38, bright CD123, moderate expressions of CD303 and CD304, and bright HLA-DR, without CD56 and CD64 expression (**Figure 8-A and B**). This pattern remains consistent across all evaluated normal control cases, providing a benchmark for distinguishing CD56+ reactive pDCs when present simultaneously, expressing positive CD2 (100%), negative CD7 (100%), and uniformly bright CD38 similar to the previous study (**Figures 8-C and 11-B**).

**Discerning CD56+ neoplastic pDCs in BPDCN**:

Our findings indicates that CD56+ neoplastic pDCs in BPDCN present with a notable decrease in CD38 and CD123 (normal pDCs vs. BPDCN cells $p$ <0.001 for both CD38 and CD123; CD56+ reactive pDCs vs. BPDCN cells $p < 0.001$ and $p$ <0.05 for CD38 and CD123, respectively), with increase in HLA-DR expression, distinguishing them from both normal and CD56+ reactive pDCs (**Figures 9 and 10; Table 5**). The co-expression of CD303 and CD304 in neoplastic pDCs were consistent at a moderate to dim intensity, validating their role as pDC-specific markers. Intriguingly, the expression profiles of CD2 and CD7 in neoplastic BPDCN cells present a more complex landscape than that observed in reactive CD56+ pDCs. Neoplastic pDCs demonstrated variability with interesting antigenic expression patterns including either CD2-/CD7 or CD2+/CD7-, while reactive CD56+ pDCs exhibit a consistent expression of these markers (CD2+/ CD7-). Our findings resonate with previous investigations, suggesting that the heterogeneity within BPDCN cells could have significant implications for disease characterization and progression.[19,23] It prompts a further exploration into how these antigenic profiles may correlate with molecular features.

Given the ongoing research and anticipation around CD123-targeted therapy for BPDCN, our optimized 12-color pDC assay hold potential as a robust method for monitoring disease progression and therapy response.[24,25] Therefore, the inclusion of CD303 and CD304 provided added specificity and ability to interpret complex post-therapy immunophenotypes, positioning the pDC assay as a powerful tool for ensuring robust and precise post-therapy assessments.

**Conclusion**

The development and optimization of monocytic and pDC assays by MFC provided an in-depth assessment of monocytic cells and pDCs. The strategic inclusion of novel markers complemented by the proven utility of established markers provided significant diagnostic advances, particularly in the context of M-AML and BPDCN. Through comprehensive immunophenotypic analysis, our study provides critical insights that could reshape current diagnostic methods, offering a more refined and comprehensive understanding of these cell types in various disease states. This allows for a deeper and more intricate understanding of immunophenotypic alterations in different pathological conditions. Looking forward, our study lays a foundation for further investigations into the implications of these findings, particularly in the context of targeted therapeutic strategies. By examining deeper into this area, we can aim to uncover novel aspects of pathophysiology, which could be pivotal in advancing our understanding and treatment of these complex conditions. In essence, the optimized monocytic and pDC provide a path towards more accurate, timely, and individualized patient care in the ever-evolving landscape of hematopathology.

## REFERENCES


1. Wood BL, Cherian S, Borowitz MJ. The Flow Cytometric Evaluation of Hematopoietic Neoplasia. In: *Henry's Clinical Diagnosis and Management by Laboratory Methods*. 24th ed. Elsevier; 2022:689-707.

2. Lacombe F, Béné MC. Flow Cytometry in Clinical Haematopathology: Basic Principles and Data Analysis of Multiparameter Data Sets. In: *Multiparameter Flow Cytometry in the Diagnosis of Hematologic Malignancies*. 1st ed. Cambridge University Press; 2018:1-13.

3. van Dongen JJM, Lhermitte L, Böttcher S, et al. EuroFlow antibody panels for standardized n-dimensional flow cytometric immunophenotyping of normal, reactive and malignant leukocytes. *Leukemia*. 2012;26(9):1908-1975. doi:10.1038/leu.2012.120

4. Matarraz S, Almeida J, Flores-Montero J, et al. Introduction to the diagnosis and classification of monocytic-lineage leukemias by flow cytometry. *Cytometry B Clin Cytom*. 2017;92(3):218-227. doi:10.1002/cyto.b.21219

5. Xu Y, McKenna RW, Wilson KS, Karandikar NJ, Schultz RA, Kroft SH. Immunophenotypic identification of acute myeloid leukemia with monocytic differentiation. *Leukemia*. 2006;20(7):1321-1324. doi:10.1038/sj.leu.2404242

6. Patnaik MM. How I diagnose and treat chronic myelomonocytic leukemia. *Haematologica*. 2022;107(7):1503-1517. doi:10.3324/haematol.2021.279500

7. Garnache-Ottou F, Vidal C, Biichlé S, et al. How should we diagnose and treat blastic plasmacytoid dendritic cell neoplasm patients? *Blood Adv*. 2019;3(24):4238-4251. doi:10.1182/bloodadvances.2019000647

8. Khoury JD, Solary E, Abla O, et al. The 5th edition of the World Health Organization Classification of Haematolymphoid Tumours: Myeloid and Histiocytic/Dendritic Neoplasms. *Leukemia*. 2022;36(7):1703-1719. doi:10.1038/s41375-022-01613-1

9. Arber DA, Orazi A, Hasserjian RP, et al. International Consensus Classification of Myeloid Neoplasms and Acute Leukemias: integrating morphologic, clinical, and genomic data. *Blood*. 2022;140(11):1200-1228. doi:10.1182/blood.2022015850

10. Selimoglu-Buet D, Wagner-Ballon O, Saada V, et al. Characteristic repartition of monocyte subsets as a diagnostic signature of chronic myelomonocytic leukemia. *Blood*. 2015;125(23):3618-3626. doi:10.1182/blood-2015-01-620781

11. Churchill HRO, Fuda FS, Xu J, et al. Leukocyte immunoglobulin-like receptor B1 and B4 (LILRB1 and LILRB4): Highly sensitive and specific markers of acute myeloid leukemia with monocytic differentiation. *Cytometry B Clin Cytom*. 2021;100(4):476-487. doi:10.1002/cyto.b.21952

12. Chen X, Wood BL, Cherian S. Immunophenotypic Features of Myeloid Neoplasms Associated with Chromosome 7 Abnormalities. *Cytometry B Clin Cytom*. 2019;96(4):300-309. doi:10.1002/cyto.b.21775

13. Dobrowolska H, Gill KZ, Serban G, et al. Expression of immune inhibitory receptor ILT3 in acute myeloid leukemia with monocytic differentiation. *Cytometry B Clin Cytom*. 2013;84B(1):21-29. doi:10.1002/cyto.b.21050

14. Clark GJ, Ju X, Azlan M, Tate C, Ding Y, Hart DNJ. The CD300 molecules regulate monocyte and dendritic cell functions. *Immunobiology*. 2009;214(9):730-736. doi:10.1016/j.imbio.2009.06.004

15. McDonnell MH, Smith ET, Lipford EH, Gerber JM, Grunwald MR. Microgranular acute promyelocytic leukemia presenting with leukopenia and an unusual immunophenotype. *Hematol Oncol Stem Cell Ther*. 2017;10(1):35-38. doi:10.1016/j.hemonc.2015.12.004

16. Swerdlow SH, Campo E, Harris NL, et al. *WHO Classification of Tumours of Haematopoietic and Lymphoid Tissues*. Revised 4th Edition. International Agency for Research on Cancer (IARC); 2017.

17. Sweet K. Blastic plasmacytoid dendritic cell neoplasm: diagnosis, manifestations, and treatment. *Curr Opin Hematol*. 2020;27(2):103-107. doi:10.1097/MOH.0000000000000569

18. Chen X, Cherian S. Acute Myeloid Leukemia Immunophenotyping by Flow Cytometric Analysis. *Clin Lab Med*. 2017;37(4):753-769. doi:10.1016/j.cll.2017.07.003

19. Wang W, Khoury JD, Miranda RN, et al. Immunophenotypic characterization of reactive and neoplastic plasmacytoid dendritic cells permits establishment of a ten-color flow cytometric panel for initial workup and residual disease evaluation of blastic plasmacytoid dendritic cell neoplasm. *Haematologica*. 2020;106(4):1047-1055. doi:10.3324/haematol.2020.247569

20. Mair F, Liechti T. Comprehensive Phenotyping of Human Dendritic Cells and Monocytes. *Cytometry A*. 2021;99(3):231-242. doi:10.1002/cyto.a.24269

21. Deng M, Gui X, Kim J, et al. LILRB4 signalling in leukaemia cells mediates T cell suppression and tumour infiltration. *Nature*. 2018;562(7728):605-609. doi:10.1038/s41586-018-0615-z

22. John S, Chen H, Deng M, et al. A Novel Anti-LILRB4 CAR-T Cell for the Treatment of Monocytic AML. *Mol Ther J Am Soc Gene Ther*. 2018;26(10):2487-2495. doi:10.1016/j.ymthe.2018.08.001

23. Wang W, Xu J, Khoury JD, et al. Immunophenotypic and Molecular Features of Acute Myeloid Leukemia with Plasmacytoid Dendritic Cell Differentiation Are Distinct from Blastic Plasmacytoid Dendritic Cell Neoplasm. *Cancers*. 2022;14(14):3375. doi:10.3390/cancers14143375

24. Cai T, Gouble A, Black KL, et al. Targeting CD123 in blastic plasmacytoid dendritic cell neoplasm using allogeneic anti-CD123 CAR T cells. *Nat Commun*. 2022;13:2228. doi:10.1038/s41467-022-29669-8

25. Pemmaraju N, Lane AA, Sweet KL, et al. Tagraxofusp in Blastic Plasmacytoid Dendritic-Cell Neoplasm. *N Engl J Med*. 2019;380(17):1628-1637. doi:10.1056/NEJMoa1815105